Electronic structure and magnetization of Fe–Co alloys and multilayers

C. Paduani and J. C. Krause

Citation: Journal of Applied Physics **86**, 578 (1999); doi: 10.1063/1.370769
View online: http://dx.doi.org/10.1063/1.370769
View Table of Contents: http://scitation.aip.org/content/aip/journal/jap/86/1?ver=pdfcov
Published by the AIP Publishing

Electronic structure and magnetization of Fe–Co alloys and multilayers

C. Paduani
Departamento de Física, Universidade Federal de Santa Catarina, UFSC, Florianópolis CEP 88040-900, SC, Brasil

J. C. Krause
Instituto de Física, Universidade Federal do Rio Grande do Sul, UFRGS, Porto Alegre CEP 91501-970, RGS, Brasil

(Received 10 November 1998; accepted for publication 11 January 1999)

The magnetic properties and electronic structure of bcc Fe–Co alloys and multilayers are investigated with the first-principles molecular cluster discrete variational method. The density of states and the contact interactions are obtained for the central atom of each cluster. Besides the local magnetic moment and the isomer shift the occupancies of $3d$, $4s$, and $4p$ shells are investigated when Co atoms are introduced in the immediate vicinity of iron sites. The calculations indicate a varying magnetic moment for Fe atoms and a constant value for Co atoms which is in agreement with experiments. For the superstructures, our results indicate a strong dependence of the local moment, contact field, and isomer shift for Fe atoms with the thick of iron layers. The internal field increases for thicker Fe layers while the local moment decreases which is also in accordance with experimental predictions. © *1999 American Institute of Physics.* [S0021-8979(99)01608-4]

I. INTRODUCTION

Over the years, the magnetic properties of the bcc phase of Fe–Co alloys have been investigated by means of several theoretical[1–7] and experimental techniques,[8–15,17,18] mostly concerning the dependence of the bulk magnetization with composition as well as the ordering–disordering process. For cobalt content up to about 0.7 at. %, these alloys form a solid solution with B2 structure. The Fe–Co alloys have an extremely high Curie temperature and the highest saturation induction at room temperature; 24.5 kG at 35 at. % Co, which deviates from the Slater–Pauling curve. Higher permeability and lower values of saturation induction are obtained in equiatomic alloys, because of their low magnetocrystalline anisotropy. These alloys exhibit face-centered-cubic (fcc) structures above 912–986 °C at about 70 at. % Co, whereas the low-temperature structure is body-centered-cubic (bcc).

In earlier studies, the magnetic behavior of these alloys with composition was explained with the additivity of the contributions from solutes in the nearest shells of neighbors around an iron atom, which worked reasonably well in dilute samples.[8,11–13,16] Further improvements in the experimental[15,18–20] and theoretical[21,5–7] works were attempted in order to describe the observed results and the somewhat unusual physical properties of this alloy system. The concentration dependence of the saturation magnetization has been interpreted as a transition from weak to strong ferromagnetism in the range of composition up to 30 at. % Co.[15]

Band-structure calculations using the augmented-spherical-wave method were performed in the bcc FeCo (equiatomic), in the local-spin-density approximation (LSDA), to study the behavior of the magnetic moment and the equilibrium lattice constants.[5] The results indicate that the average magnetic moment does not vary linearly with composition, and the observed increase is caused by an increase of the local iron moment, while the cobalt moment remains constant. The magnetic properties of disordered Fe–Co alloys have been also calculated by using a tight-binding scheme in a single-site approximation, employing the Slater–Koster parametrized method.[6] The calculations indicated that the magnetization of the alloys at the cobalt-rich side depends on the number of available d holes, while for the iron-rich alloys it is influenced by a weak electron–electron interaction, being that the intersection of these two effects occurs at about 30 at. % Co, where it produces the sharpest maximum on the Slater–Pauling curves.

The local density of $3d$ electrons at Fe atoms in different concentrations in Fe–Co alloys were investigated by Hamdeh *et al.*, by electron-energy-loss spectrometry (EELS).[15] According to their results, the change in the total number of $3d$ electrons at the iron atoms was much smaller than the increase in the μ value, which indicated changes in the population of both spin-up and spin-down bands. Besides, the magnetic moment increased from $2.22\mu_B$ in pure iron to about $3.0\mu_B$ at 70 at. % Co. In fact, the results showed that the average number of spin-up $3d$ electrons increases in this concentration range, whereas the spin-down occupancy decreases, together with the $4s$ population. Moreover, the average hyperfine field increases steadily up to about 20 at. % Co. A disordered crystalline solid solution of Fe–Co can also be formed by mechanical alloying.[18] The saturation magnetization measured in the samples so obtained is proportional to the average hyperfine magnetic field, which increases with the addition of cobalt in the matrix of bcc iron. The current interpretation of the observed results is that the increase in the mean magnetic moment is due to the increase of the magnetic moment at the Fe atoms, while the Co atoms should maintain a constant μ value at about $1.85\mu_B$.[15,17]

General-potential linear augmented plane wave (LAPW) calculations of the electronic structure in equiatomic Fe–Co was performed by Liu and Singh[7] in order to investigate in which extent the LSDA considering spherical approximations for the potential was responsible for the observed discrepancies between polarized-neutron-scattering studies and the first-principles calculations of Schwarz and Salahub.[5] The lattice parameter obtained for the equiatomic FeCo is slightly smaller (3%) than the measured value. Besides, although this treatment gives some improvement regarding the asphericity of the spin density some differences still remains, which lead them to conclude as being a underestimation of the LSD approach. One feature pointed out in this work is, as the radius of the atomic sphere is increased from 2.15 to 2.3 a.u., the amount of interstitial charge decreases from about 2.9 to 2.1 electrons per cell, whereas the spin polarizations within the spheres change by less than 0.02 electrons, which reflects the fact that the moments arise from the polarization of the $3d$ orbitals. Indeed, the calculations also confirmed an enhancement of the Fe moment in this composition over the bcc iron, while the Co moment is similar to the value in hexagonal-close-packed (hcp) Co.

Multilayer films consisting of ferromagnetic elements also have attracted much attention because of high magnetic flux density. More recently molecular beam epitaxy (MBE) grown Co/Fe superlattices with thickness varying in the range from 5 to 42 Å have been grown on GaAs(110) substrates.[22] The x-ray diffraction (XRD) and nuclear magnetic resonance (NMR) analysis of the chemical short range order confirm that cobalt can be stabilized in a bcc structure up to a critical thickness of 21 Å. Fe–Co films deposited in an alternating multilayer structure were also obtained by a magnetron dc-sputtering method, which have an artificial superlattice structure with crystallographic coherence between constituent layers.[23] The films so obtained are bcc with (110) planes parallel to the film surface and its lattice constant is smaller than for bulk iron, and decreases linearly to about 2.81 Å with increasing cobalt layer thickness. The films are ferromagnetic with an easy magnetization direction in the film plane. In comparison with that of Fe–Co alloy films, the magnetization is smaller for multilayers with a thicker Fe than Co layer and larger for those with a thinner Fe than Co layer. Thus, the large magnetization of Fe–Co films is attributed to the large magnetization of bcc Co relative to bulk hcp Co.

Most of the calculations that have been done previously in Fe–Co alloy systems are concerned with ordering/disordering processes or on the description of the magnetization with cobalt concentration at the equiatomic composition or ordered phases. There is still a lack of a full description of a microscopic point of view of the hyperfine properties, such as the contact field and isomer shift, as well as how the occupancies of the $3d$ spin-down states and the s-like states depend on the cobalt concentration. In this article, we discuss the effect on the magnetic properties of replacing each atom in the immediate neighborhood of a Fe atom by Co atoms. We investigate also the dependence of the magnetic properties on the thick of iron layers in multilayered structures. In the calculations, we employ the discrete variational (DV) method[24] to obtain the electronic structure of disordered bcc Fe–Co alloys and multilayers in spin-polarized calculations in the LSD approximation. For the potential of the exchange-correlation energy is adopted the Barth–Hedin approximation.[25] Since the DV method has been described in detail in the literature listed above, we will concentrate our attention particularly on the discussion of the results of the present calculations.

II. RESULTS AND DISCUSSION

To solve the self-consistent one-particle Kohn–Sham equations, the molecular orbitals are expanded on a basis of atomic numerical orbitals, where we adopted the minimal basis, which includes $1s-4p$ orbitals for both Fe and Co. The molecular clusters representing the alloys in the bcc phase were built up with 15 atoms, including two shells of neighbors around the central atom. The known experimental value of 5.416 a.u. was used for the lattice spacing of bcc iron. The origin of coordinates is at the body centered site. For the superlattices, we used also a 15 atom cluster with the same lattice spacing as before but now with the [110] direction parallel to the z axis. Thus, the cube is rotated so that the first nearest neighborhood (NN) consists of eight atoms equidistant of the central atom, at the corners of rectangles, four in the plane $z=0$ and four in the plane $y=0$. The next nearest neighbors (NNN) are four atoms in the plane $x=0$ distant $a/\sqrt{2}$ from the origin of coordinates. Furthermore, there are two atoms in the x axis at $\pm a$. The adopted superstructures are: (i) a Fe/Co interface, where the atoms in the $z=0$ and the lower planes are Fe atoms; (ii) a Co/Fe interface, with a plane of Co atoms at $z=0$; (iii) a Fe/Co monolayer (plane Fe at $z=0$), and (iv) a multilayer, consisting of three planes of Fe(Co) atoms, with the middle plane of Fe atoms at $z=0$. The potential crystal was made up of about 400 atoms. Potential wells in the crystal region were truncated near the Fermi surface in order to prevent the migration of electrons from the cluster toward low-lying states in the crystal. The embedding scheme is well described in detail elsewhere in the literature.[26] As usual the central atom of each cluster is chosen as the probe atom which is expected to exhibit bulk-like properties.

In Fig. 1 are displayed the $3d$ partial density of states (PDOS) for the central atom representing pure bcc iron (a), for single Co impurity in bcc iron host (b), and for the cluster with eight Co NN atoms around the central iron atom (c). As one observes in Fig. 1(a) the majority PDOS are entirely fulfilled and the hole states are in the spin-down band as expected, whereas the Fermi energy falls into a minimum of the minority-spin DOS. For the single Co atom, Fig. 1(b) shows a sharp resonance just at the Fermi energy for spin-up states (which indicates that these electrons indeed give the major contribution for the electronic specific heat coefficient γ, $C_c(T)=\gamma T$) and another one above it for spin-down states. However, in spite of the high intensity of this peak the topological features of this PDOS are similar to that for pure bcc Fe showed in Fig. 1(a). The smaller exchange splitting for Co is also clear in Fig. 1(b), with a high peak at E_F which forms a partially occupied bound state. Moreover, the $3d$

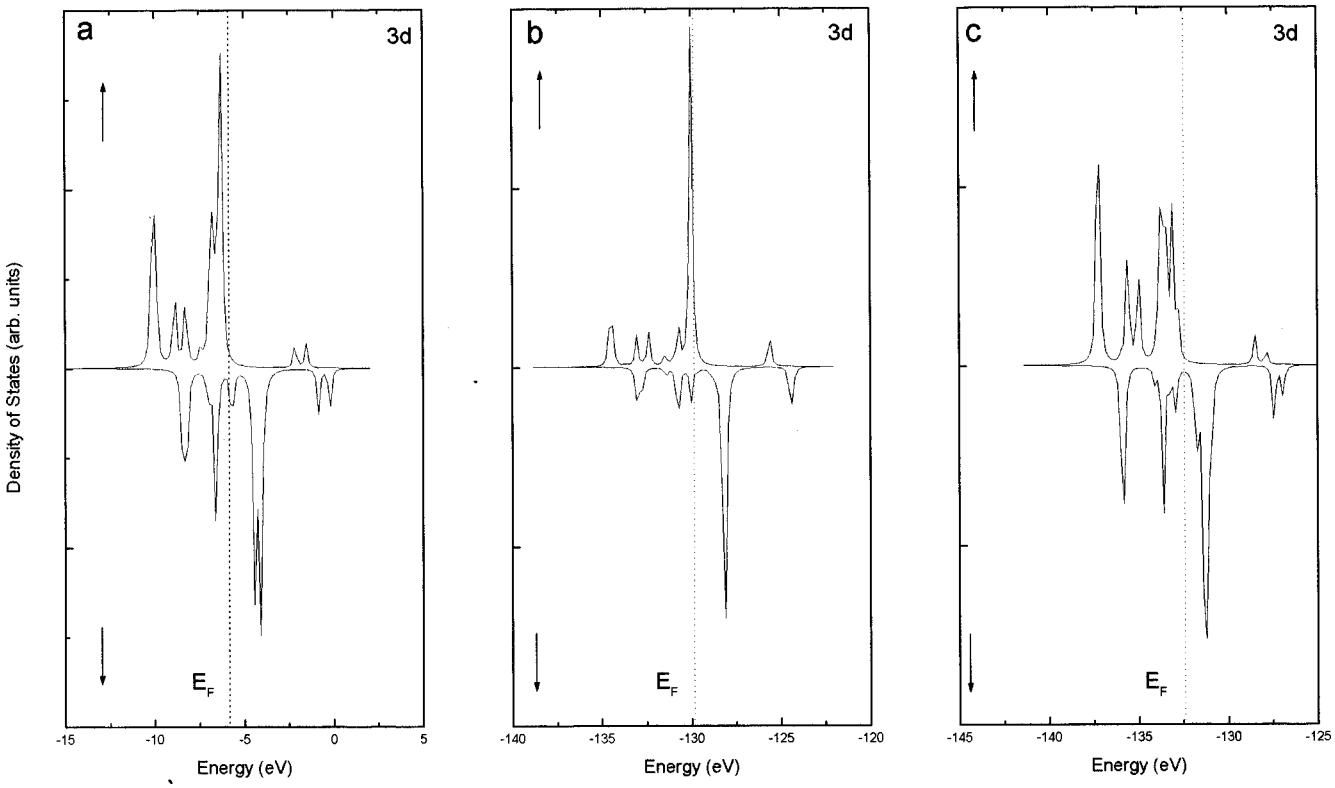

FIG. 1. 3*d* PDOS for: (a) pure bcc iron; (b) a single Co impurity, and (c) a Fe atom with eight Co NN atoms.

states are well localized in the energy space, and a small peak is also observed just at the Fermi energy for the 3*d* spin-down states. The lower-lying occupied spin-down states are separated from the higher antibonding states by a minimum just above the Fermi surface, as is typical for bcc metals. The ordered equiatomic condition is represented by the cluster with eight Co NN atoms around the central iron atom, whose PDOS are showed in Fig. 1(c). This result is in agreement with earlier calculations, which have shown that the majority-spin 3*d* states are fully occupied and a very prominent peak appears above the Fermi surface for both Fe and Co atoms for minority spins in this case.[7] In fact, by comparing the Figs. 1(a) and 1(c) one observes very similar features between these diagrams. It has been pointed out before that Fe is magnetically weak because of an insufficient electron–electron interaction to the bandwidth ratio, while in disordered FeCo this interaction for the Co atoms could assists the weaker interaction in Fe in saturating the bulk magnetization.[6] This should arise from the enhancement of the exchange splitting relative to pure Fe, as can be observed in these diagrams, which confirms indeed that equiatomic FeCo is a strong ferromagnet.

In Figs. 2 and 3 are displayed the 3*d* PDOS for the superstructures. For the Fe atom at the interface, Fig. 2(a) shows some loss of structure in the 3*d* subbands, whereas for the Co atom at the interface showed in Fig. 2(b) one observes a high peak just above the Fermi surface for the spin-down 3*d* hole states. Observing these diagrams, one can see how the majority-spin 3*d* PDOS for both Fe and Co atoms at the interface are very similar. However, the 3*d* minority-spin PDOS for the Co atom showed in Fig. 2(b) has more weight than that for Fe, owing to the extra electron for Co, which in turn has a lower value to the magnetic moment. In Fig. 3(a) one can verify that for Fe atoms in a monolayer the 3*d* spin-up states are more spread out in energy, as well as a bonding character for the spin-down states. For the multilayer, in Fig. 3(b) is clearly observed a loss of coupling for the 3*d* electrons of Fe atoms in the middle plane and an increase of the population of spin-down *d* electrons, which in turn should decrease the local moment.

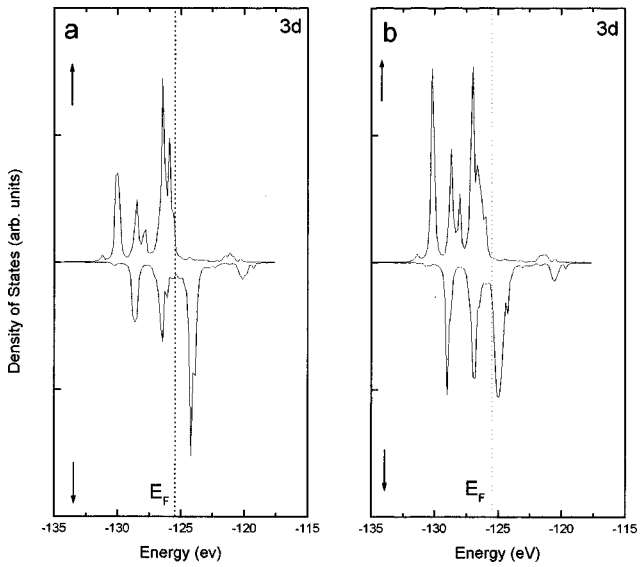

FIG. 2. 3*d* PDOS for: (a) a Fe atom at a Fe/Co interface; (b) a Co atom at a Co/Fe interface.

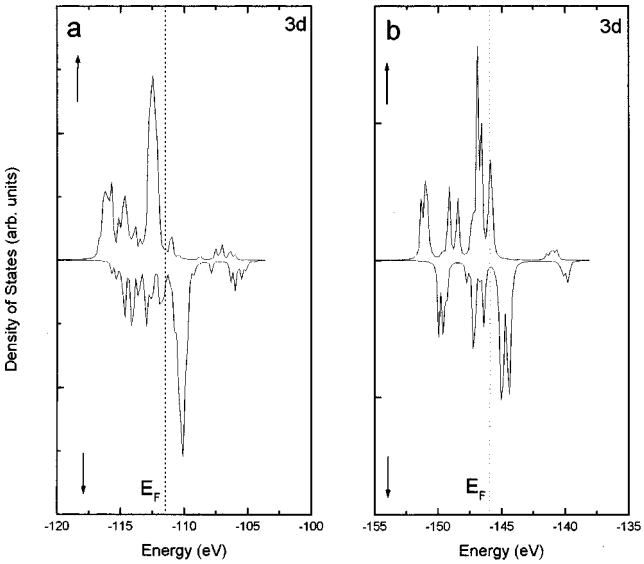

FIG. 3. $3d$ PDOS for a Fe atom: (a) in a monolayer, and (b) at a middle plane in a multilayer of three planes of Fe(Co) atoms.

In Table I are shown the partial charges for the central iron atoms obtained in the present calculations. As one observes, our results show that in Fe–Co alloys the iron $3d$ population for spin-up electrons increases with the addition of Co atoms in the first shell of neighbors around an iron atom. Thus, the observed increase of the μ value at the equiatomic composition arises from both the increase of the contribution from spin-up electrons in this subband and from the decrease of the population of the spin-down states, relative to pure iron. The contribution from spin-up conduction electrons for the local moment of Co is similar to that for Fe, as one should expect considering that Co is magnetically saturated. The local symmetry plays a minor rule for the orbital populations, as can be checked out in the table.

The calculated magnetic properties are listed in Table II. As one verifies, the local symmetry has no effect on the local moment. Besides, the conduction band contribution is always negative, and has opposite variation to that coming from d electrons. The Co atom as a single impurity in this host

TABLE I. Calculated electronic distribution in the different subbands for each cluster.

Cluster	$3d_\uparrow$	$3d_\downarrow$	$4s_\uparrow$	$4s_\downarrow$	$4p_\uparrow$	$4p_\downarrow$
$FeFe_8Fe_6$	4.5421	1.9027	0.2885	0.4489	0.2502	0.4377
$CoFe_8Fe_6$	4.7800	2.5891	0.3274	0.5003	0.2773	0.6023
$FeFe_2Co_1Fe_6$	4.3099	2.3318	0.3532	0.4825	0.2628	0.5021
$FeFe_6Co_2Fe_6$[a]	4.5495	1.9712	0.3336	0.4595	0.2958	0.5263
$FeFe_6Co_2Fe_6$[b]	4.5349	1.9827	0.3429	0.4527	0.3017	0.5211
$FeFe_4Co_4Fe_6$[c]	4.6423	1.8633	0.3593	0.4558	0.3114	0.5127
$FeFe_4Co_4Fe_6$[d]	4.6001	1.9117	0.3551	0.3196	0.4374	0.5076
$FeCo_8Fe_6$	4.7158	1.8027	0.3383	0.3668	0.2568	0.3648
$FeFe_8Co_6$	4.6225	1.9513	0.3321	0.4343	0.2857	0.4516
$FeFe_8Fe_6Co_1$	4.2693	2.2403	0.3575	0.4800	0.3056	0.5798

[a] D_{3d}
[b] C_{2v}
[c] T_d
[d] D_{2d}

TABLE II. Calculated parameters for the central atom: total magnetic moment (μ), the contribution from the conduction band $4s+4p$ (μ_c), the charge transfer (Q), the contact field (H_c), and the isomer shift (IS), relative to α-iron. α-Fe means pure bcc iron in another type of cluster, adopted for the superstructures. The multilayer results account for Fe atoms in a superstructure consisting of three planes of Fe(Co) atoms.

Cluster	μ	μ_c	Q	H_c(kG)	IS(mm/s)
$FeFe_8Fe_6$	2.29	−0.35	0.17	−347	⋯
$CoFe_8Fe_6$	1.65	−0.47	−0.11	−465	⋯
$CoFe_7Co_1Fe_6$	1.27	−0.40	−0.06	−449	⋯
$FeFe_7Co_1Fe_6$	1.61	−0.37	−0.19	−425	0.14
$FeFe_6Co_2Fe_6$[a]	2.22	−0.35	−0.10	−476	0.06
$FeFe_6Co_2Fe_6$[b]	2.22	−0.33	−0.10	−458	0.06
$FeFe_4Co_4Fe_6$[c]	2.48	−0.30	−0.11	−462	0.06
$FeFe_4Co_4Fe_6$[d]	2.42	−0.27	−0.09	−457	0.06
$FeCo_8Fe_6$	2.72	−0.20	−0.08	−420	0.06
$FeFe_8Co_6$	2.40	−0.31	−0.07	−405	0.03
$FeFe_8Fe_5Co_1$	1.63	−0.39	−0.19	−427	0.03
$\alpha-Fe$	2.26	−0.29	0.14	−320	⋯
Fe/interface	2.18	−0.28	−0.04	−419	0.07
Co/interface	1.87	−0.24	0.01	−374	⋯
monolayer	2.57	−0.18	0.09	−406	0.10
multilayer	1.62	−0.40	−0.34	−470	0.01

[a] D_{3d}
[b] C_{2v}
[c] T_d
[d] D_{2d}

shows a μ value close to hcp Co ($1.75\mu_B$); the experimental results is about $1.7\mu_B$.[6] The addition of one Co atom in the first neighborhood reduces the local moment at the central Co atom to $1.27\mu_B$. In fact, experimental results have indicated that in dilute alloys the Co atoms do not fill randomly the lattice, since Co avoids to have Co first neighbors.[11] With one Co NN atom, the central iron moment decreases to $1.61\mu_B$, coming up mostly from the reduction of the spin-up $3d$ eletrons, which are being transfered to the spin-down subband; for the Co atom in this cluster, we obtained $\mu = 1.84\mu_B$. Since there, the iron moment increases steadly up to $2.78\mu_B$ for eight Co NN atoms (where $\mu_{Co}=1.83\mu_B$), which is in good agreement with the experimental predictions. With two(four) Co NN atoms we obtained $1.82(1.80)\mu_B$ for the local moment at the Co atoms; so our results also confirm a constant value for the magnetic moment of Co atoms in this matrix. The μ_c contribution decreases in the table to a minimum for eight Co NN atoms. Besides, one Co NNN atom causes the same effect on the local moment at the central iron atom as a substitution in the first neighborhood. In the table one sees also that the Fe atom at the interface shows a small reduction of the local moment relative to bulk atoms, whereas the Co atom have an enhanced value over the pure cobalt. For a monolayer, the Fe atoms exhibit a larger μ value, besides a smaller contribution of the conduction electrons to the local moment. Finally, in the middle plane of three planes of iron atoms in a multilayered structure is observed a lower value of the magnetic moment at Fe atoms. These features are confirmed by experimental results.[23,27]

The Q value in Table II shows the charge transfer in each case. The Co atom isolated in bcc iron host acts as an atractor for electrons. Nevertheless, the presence of one Co

NN atom decreases the ionization at the central Fe atom, which also changes signal. The further addition of Co atoms in its immediate vicinity causes an inflow of electrons into the iron site, which is decreasing as more solute atoms are being added. Besides, the addition of one Co NNN atom brings out the same disturbance in the charge transfer as a replacement in the first shell of neighbors around the central iron atom. However, for the ordered situation with the second shell of neighbors completely filled up with cobalt atoms, the central iron site has a small ionization. Because Co is more electronegative than Fe the ionization of the iron site is quite sensitive to the local atomic arrangement in this matrix. Furthermore, for the iron atoms at the interface is observed a small ionization, whereas the Co atoms do not suffer any charge transfer in this case. In the other hand, there is a striking difference between the Q values for the monolayer and the multilayer.

The contribution of the core orbitals to the contact field (H_c) are obtained by means of a atomic calculation in the X_a approximation, by using the converged electronic configurations from the molecular calculations, after an appropriate diagonal weighed population analysis in order to obtain the atomic orbital populations. This treatment is advisable considering the finite cluster size. The conduction electrons contribution is obtained directly from the molecular orbitals. In Table II one sees that H_c is always negative and quite sensitive to the local symmetry in this matrix. This contact field increases steadily up to the addition of four Co atoms in the immediate neighborhood of iron sites. At the equiatomic composition, our results indicate that a reduction of the internal field is expected due to the lowest contribution from the $4s$ electrons in this case, which has the same signal to that from the deep core electrons which gives the main contribution to the local field. For six Co NNN atoms is observed a reduction of the contact field, which arises from the reduction of the contribution from localized electrons to the spin density at iron nuclei. It has been pointed out before from band-structure calculations that the loss of spin-down $4s$ electrons upon alloying is responsible to the difference between calculated and experimental results for the contact field.[15] This occupancy should decrease with cobalt concentration, thus giving decreasing field values, which are negative and have the same signal of the contribution from the conduction electrons to the spin density at iron nuclei. The $3d$ spin-down antibonding states formed during alloying are repulsed to higher energy, pulling together the spin-down $4s$ states through the exchange interactions. The overall change in the $4s$ occupancy with alloying have a small contribution of spin-up $4s$ population. Moreover, one Co NNN causes the same effect in the H_c value at the iron nucleus as when it occupies the first coordination sphere, thus confirming a somewhat long range order mechanism in this case. Nevertheless, the highest H_c value is not occurring when the saturation of the magnetization takes place, and no linear correlation exists between them. The changes occurring in the local field are mostly due to the variation of the core eletron-s spin density at iron nuclei, which is quite sensitive to the occupancy of the neighboring shells by Co atoms. Finally, for both Co and Fe atoms at the interface, in Table II one can see larger values for the contact field, as well as larger values for H_c for multilayers with a thicker Fe layer.

Contrary to the contact field, the isomer shift is practically insensitive to the introduction of Co atoms in the first neighborhood of the iron sites at 0 K. All calculated IS values are positive, in accordance with experimental results from Mössbauer spectrometry.[15] With the occupancies by Co atoms in the second shell of neighbors the IS values are even smaller, although they are closer to the experimental results at room temperature. In fact, it is known from experimental results that for a disordered alloy with 30 at. % Co, IS increases from 0.03 mm/s at room temperature up to about 0.045 mm/s at 77 K, and is constant up to 40 at. % Co, decreasing thereafter to 0.04 mm/s at 50 at. % Co.[11,15] However, for the superstructures IS is strongly dependent on the thick of iron layers, as can be seen in Table II, and keep a positive value too. Although these results are holding for 0 K, one should keep in mind also that the effect of the cobalt concentration on lattice spacing is not being considered in the present calculations, which has a profound effect on the calculated hyperfine properties such as H_c and IS. It is known that the magnitude of the contact field decreases upon ordering, an effect which is also confirmed by our calculations. Actually, another feature depicted from these results is that one should be very careful about the nonlocal contributions to the contact field in order to understand the changes occurring during alloying. However, our results are primarily concerned with the behavior of those quantities with composition through a microscopic description, and a good agreement of these trends with the experimental results is achieved.

In summary, we have performed first-principles calculations in LSDA to study local magnetic properties and the electronic structure of disordered Fe–Co alloys and multilayers. In brief, the average magnetic moment increases due to the increase of the polarization of the iron d orbitals, besides the changes in the population of both spin-up and spin-down $4s$ subbands. The local Co magnetic moment is about the same as in pure bcc cobalt, whereas the local iron moment increases with the cobalt concentration. In equiatomic FeCo an enhanced moment is obtained over the pure bcc iron value. The local spin DOS for the equiatomic alloy shows a fully occupied $3d$ subband, whereas the $4s$ minority states has a strong effect on the enhancement of the iron moment. The saturation of the magnetization should arises from the increase of the effective electron-electron interaction in the iron atoms. For the multilayers, our results predict a strong dependence for Fe atoms of the local moment, contact field and isomer shift with the thick of iron layers. Actually, the calculated internal field increases for thicker Fe layers, which is in accord with the experimental results. The hyperfine field of iron in the interface monolayers in the magnetic multilayers is found to be substantially reduced compared with that in the corresponding bulk metal, in strong contrast to the highly enhanced magnetic moments in the same monolayers.

ACKNOWLEDGMENTS

The authors thank the NPD of UFSC for the computational support. This work was supported by CNPq and Finep, Brazilian agencies.

[1] R. Richter and H. Eschrig, J. Phys. F **18**, 1813 (1988).
[2] H. Hasegawa and J. Kanamori, J. Phys. Soc. Jpn. **33**, 1607 (1972).
[3] N. Hamada, J. Phys. Soc. Jpn. **46**, 1759 (1979).
[4] J. Kaspar and D. R. Salahub, J. Phys. F **13**, 311 (1983).
[5] K. Schwarz and D. R. Salahub, Phys. Rev. B **25**, 3427 (1982); K. Schwarz, P. Mohn, P. Blaha, and J. Kubler, J. Phys. F **14**, 2659 (1984).
[6] R. H. Victora and L. M. Falicov, Phys. Rev. B **30**, 259 (1984); R. H. Victora, L. M. Falicov, and S. Ishida, *ibid.* **30**, 3896 (1984).
[7] A. Y. Liu and D. J. Singh, Phys. Rev. B **46**, 11145 (1992).
[8] G. K. Wertheim, Phys. Rev. B **1**, 1263 (1970).
[9] D. I. Bardos, J. Appl. Phys. **40**, 1371 (1969).
[10] M. F. Collins and J. B. Forsyth, Philos. Mag. **8**, 401 (1963).
[11] I. Vincze, I. A. Campbell, and A. J. Meyer, Solid State Commun. **15**, 1495 (1974).
[12] B. de Mayo, Phys. Rev. B **24**, 6503 (1981).
[13] G. K. Wertheim, V. Jaccarino, J. H. Wernick, and D. N. E. Buchanam, Phys. Rev. Lett. **12**, 24 (1964).
[14] D. H. Pearson, B. Fultz, and C. C. Ahn, Appl. Phys. Lett. **53**, 1405 (1988).
[15] H. H. Hamdeh, B. Fultz, and D. H. Pearson, Phys. Rev. B **39**, 11233 (1989).
[16] M. B. Stearns, Phys. Rev. B **9**, 2311 (1974).
[17] E. Di Fabrizio, G. Mazzone, C. Petrillo, and F. Sacchetti, Phys. Rev. B **40**, 9502 (1989).
[18] R. Brüning, K. Samwer, C. Kuhrt, and L. Schultz, J. Appl. Phys. **72**, 2978 (1992).
[19] Y. Iijima and C-G. Lee, Acta Metall. Mater. **43**, 1183 (1995).
[20] Ö. F. Bakkaloglu, M. F. Thomas, R. J. Pollard, and P. J. Grundy, J. Magn. Magn. Mater. **126**, 261 (1993).
[21] B. Drittler, N. Stefanou, S. Blügel, R. Zeller, and P. H. Dederichs, Phys. Rev. B **40**, 8203 (1989).
[22] J. P. Jay, E. Jedryka, M. Wojcik, J. Dekoster, G. Langouche, and P. Panissod, Z. Phys. B **101**, 329 (1996).
[23] N. Sato, J. Appl. Phys. **67**, 4462 (1990).
[24] D. E. Ellis, Int. J. Quantum Chem. **2S**, 35 (1968); D. E. Ellis and G. S. Painter, Phys. Rev. B **2**, 2887 (1970); G. S. Painter and D. E. Ellis, *ibid.* **1**, 4747 (1970); E. J. Baerends, D. E. Ellis, and P. Ros, Chem. Phys. **2**, 41 (1973).
[25] U. von Barth and L. Hedin, J. Phys. C **5**, 1629 (1972).
[26] B. Delley and D. E. Ellis, J. Chem. Phys. **76**, 1949 (1982).
[27] G. Y. Guo and H. Ebert, Phys. Rev. B **53**, 2492 (1996).